Burke: The remark was made that the LMC concentrations appeared comparable to those in the Galaxy. In McGee's study of the cloud complexes in our own Galazy, he presented two hierachies of complexes, one ranging around 100–200 pc, and the second being 1500 pc typically. The list of sizes presented here for the LMC looks more or less like a geometric mean of these values. I don't think one can say yet that these hydrogen associations are comparable.

McGee: Some clouds in the Galaxy at $R_0 = 9$–10 kpc are of the same general order in the z dimension but are extended in an approximately 2 to 1 ratio along the arms. The analogy is not complete.

Westerhout: Indeed, we should congratulate Mr. McGee and collaborators on these fine observations. But I do not agree with Dr. Bok that the scale of the radio maps is already useful for comparison with optical data. The resolving power is still of the order of 300 pc. If we see regions 300–800 pc in diameter, we do not know at all what their composition is. A fair proportion of the regions agrees not only in position, but also in size with the HII regions. One cannot of course have neutral and ionized hydrogen in the same place. Therefore, we might think of a model where, as in our Galaxy, the hydrogen in such large aggregates occurs in the form of rather dense knots with empty regions in between. In such a region there are apparently OB stars, which ionize some of the hydrogen knots. But it will take a resolution of 1 minute of arc or so before we can solve the question of the distribution of the gas over HI and HII regions.

The interesting new information in this paper is the breaking up of the formerly smooth hydrogen distribution into large separate regions. But let us not call these large regions clouds! They most likely form a very complicated structure.

63. PHOTOELECTRIC SPECTROPHOTOMETRY OF EMISSION NEBULOSITIES IN THE MAGELLANIC CLOUDS

H. R. Dickel, University of Michigan; L. H. Aller,* University of California, Los Angeles; D. J. Faulkner, Mount Stromlo Observatory

I. *Emission Nebulosities in the Large Magellanic Cloud*

Photometric measurements of the emission nebulosities in the LMC are not numerous. Doherty, Henize, and Aller (1956) microphotometered both widened and unwidened objective-prism photographs covering a narrow wavelength range near Hα to obtain cross-sectional "intensity profiles" for certain nebulosities in the Large Cloud. These intensities were converted to surface brightnesses by tracing the widened spectra of stars of known magnitude and colour and using the method of Ambartsumian (1933). Peak intensities for each scan across a nebulosity are given in erg cm^{-2} sec^{-1} steradian^{-1}.

Many of the emission nebulosities in the LMC are filamentary in structure. The classic example is 30 Doradus but other objects such as Henize 144, 159, and 160 show a pronounced fine structure. (See Figs. 1, 2, 3, and 4.) This inhomogeneity must be taken into account when we convert surface brightness into electron densities. Densities in the filaments may appreciably exceed those found from averages taken over the volume occupied by the nebula. Spectrophotometry of the emission nebulosities in the LMC was undertaken mostly at Mount Bingar with the Michigan photoelectric scanner. Throughout, we used the D slots which sufficed to

* Senior National Science Foundation (USA) post-doctoral Fellow at Australian National University, 1960–61.

admit enough light to the photocell to measure the strongest lines. Table 1 gives the data on the slot sizes, including the dimensions in seconds of arc at the focus on the slot and the area in steradians, all calculated for Bingar.

TABLE 1

SCANNER SLOTS AND APERTURES USED ON EMISSION NEBULOSITIES IN THE LARGE MAGELLANIC CLOUD

Slots	Bingar E.–W. Dimension (sec of arc)	Bingar N.–S. Dimension (sec of arc)	Bingar Slot Area in Steradians
D5	200	88	$4 \cdot 14 \times 10^{-7}$
D4	157	88	$3 \cdot 26 \times 10^{-7}$
D3	~ circular	$r = 57$	$1 \cdot 83 \times 10^{-7}$
D0	214	88	$4 \cdot 44 \times 10^{-7}$
C5	228	38	$2 \cdot 02 \times 10^{-7}$
C4	168	38	$1 \cdot 4 \times 10^{-7}$

Fig. 1.—Emission nebulosities in the Large Magellanic Cloud near 30 Doradus. This photograph was obtained with the 74-inch reflector at Mount Stromlo on Dec. 21, 1960. The photograph shows Henize nebulosities 159 and 160, which include NGC 2077, 2078, 2079, 2080, 2083, 2084, 2085, and 2086. (ORI (red) filter, 103aE emulsion, 60 min exposure.)

The observational procedure was to centre the nebulosity in the slot, using the periscope immediately behind the entrance aperture. Then the spectrum was scanned from about 5200 to 3400 Å, the direction of the grating drive reversed, and the scan repeated. By superposing direct and reverse scans, the reliability of the tracing and spectral features displayed could be assessed. In Figure 5 we compare direct and reverse scans for two nebulosities of somewhat different levels of excitation. The [OIII] λ4949 and λ5007 lines are much stronger in NGC 2040, indicating that it has a higher level of excitation.

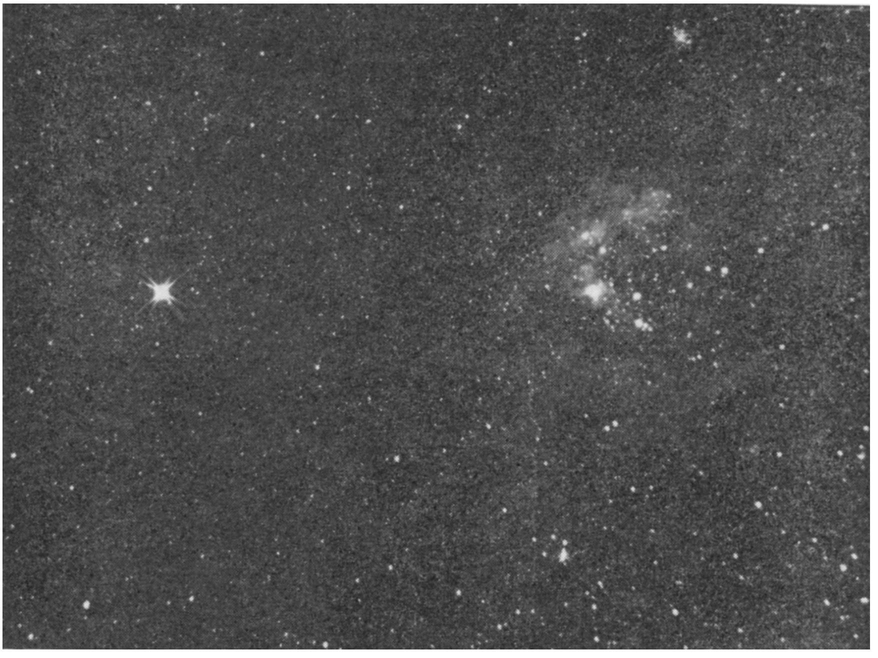

Fig. 2.—The emission nebulosity Henize 144 in the Large Magellanic Cloud photographed with the 74-inch reflector at Mount Stromlo. This object includes NGC 1962, NGC 1965, NGC 1966, and NGC 1970. (ORI filter, 103aE emulsion, 60 min exposure.)

The problem of nebular spectrophotometry can be resolved into two aspects: (1) the surface brightness in one of the monochromatic emissions, e.g. Hβ; and (2) the relative intensities of the principal nebular lines. The second problem is relatively simple; one need know only the atmospheric extinction and sensitivity function of the photocell and the transmissivity of the optics. Both of these quantities can be obtained by observing proper "comparison" stars of known energy distribution, and "extinction" of stars at different zenith distances.

The determination of the surface brightness is more troublesome in that one must compare the monochromatic radiation of, say, Hβ with the flux from a star in a unit wavelength interval at λ4861 and then determine the monochromatic magnitude of the star. Since we observed mostly stars of early spectral class whose colours differed from that of the Sun, we decided that it was better to use Willstrop's monochromatic fluxes (1960) for stars of magnitude $V = 0$ and different $(B-V)$'s rather than Ambartsumian's procedure. We observed the star and nebula with different slot sizes, i.e. spectral purities, and amplifications. We always observed the stars with B slots, i.e. 9 Å resolution. The reduction method is straightforward but involved.

The principal results are summarized in Table 2. The first column gives the number in Henize's catalogue. The second column gives the quality of the scan of Hβ.

Fig. 3.—The emission nebula near S Doradus photographed with the 74-inch reflector at Mount Stromlo Observatory in December 1960. (ORI filter, 103aE emulsion, 60 min exposure.)

For most of these nebulae, the quality was A or B, although occasionally poor deflections were obtained. Column 3 gives the slot sizes for both the entrance and exit slots. In most instances the D slots had to be used, yielding a spectral purity of 106 Å.

In many instances the nebulosities did not fill the slot. In yet others the slot was smaller than the nebula. Column 4 gives the estimated fraction of the slot area filled by nebulosity. An entry of "1" means that the nebula filled the slot. Stencils corresponding to slot sizes as reduced to the scales of appropriate photographs of the

https://doi.org/10.1017/S007418090005275X Published online by Cambridge University Press

nebulosities were used to estimate the areas actually filled by the nebulosities. Extensive notes and sketches of the nebulosities as they appeared in the slot at the time of observation also aided the making of such estimates as are entered in column 4. Column 5 gives the surface brightness in Hβ in units of 10^{-4} erg cm^{-2} sec^{-2} steradian^{-1} (averaged over the amount of the nebula in the spot). In some instances the nebulosity consisted of a bright blob on a diffuse background. For example, in Henize 69, an intense blob filling only one-tenth of the slot gives $S(\mathrm{H}\beta) = 8$ in our units; however, the average over the slot would be 1·0. In column 6 we give the ratio of the sum of

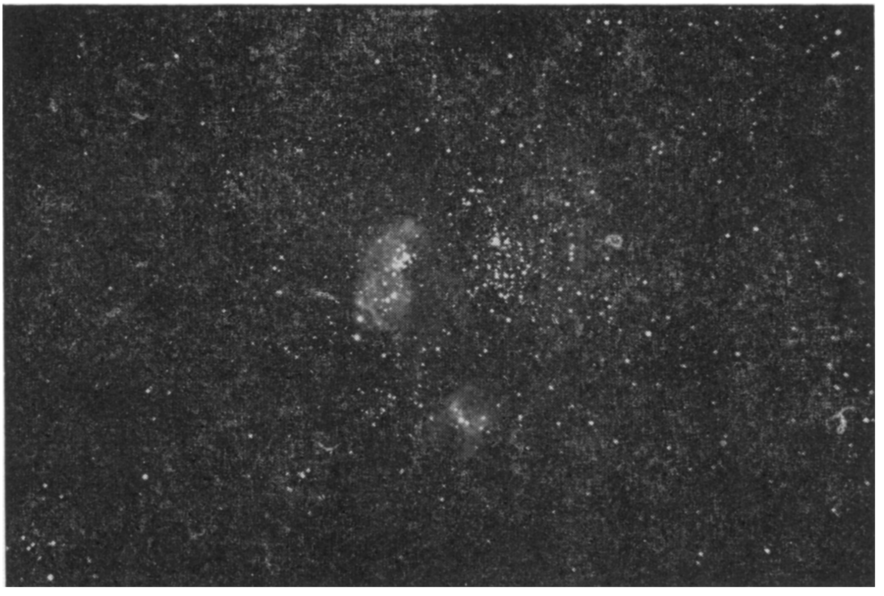

Fig. 4.—Emission nebulosities, Henize 11, in the Large Magellanic Cloud photographed with the 74-inch reflector at Mount Stromlo. This nebula includes IC 2116, NGC 1769, NGC 1763, IC 2115, NGC 1773, and NGC 1760. (ORI filter, 103aE emulsion, 60 min exposure.)

the intensities of the green nebular [OIII] lines to Hβ. From this ratio one may estimate the "excitation class" of the nebula 7. For Henize 77 the excitation class is estimated from $I(N_1+N_2)/I(\lambda 3727)$ to be 4·5. The larger the number in the last column the higher the level of excitation of the nebula (see Aller 1956, p. 66).

Table 3 gives the relative intensities of the lines observed in the various nebulosities on the scale H$\beta = 10$. To each line measured on the tracing one may assign a quality ranging from A (for good data) to E (for a line which is very poor). The lines listed are the green nebular lines $5007 + 4959 = N_1 + N_2$[OIII], H$\beta = 10$, HeI $\lambda 4472$, Hγ $\lambda 4340$, Hδ $\lambda 4101$, $\lambda 3969$ (Hϵ + [NeIII]), $\lambda 3865 + \lambda 3889$ ([NeIII] + H), $\lambda 3835$ (rarely), and $\lambda 3727$ [OII]. In all of these nebulosities the intensities of the helium lines are low and the quality of the measurements is poor. If we include all the nebulosities and take a straight average we get a He/H abundance ratio of 1 : 7, but the uncertainty is so large that this number must be regarded as meaningless.

It is best to adopt the He/H ratio from the work of Johnson (1959), or the more recent studies of D. J. Faulkner.

We now describe briefly the utilization of these data to derive ionic abundances for hydrogen, oxygen (OII and OIII), and NeIII. The methods have been adequately

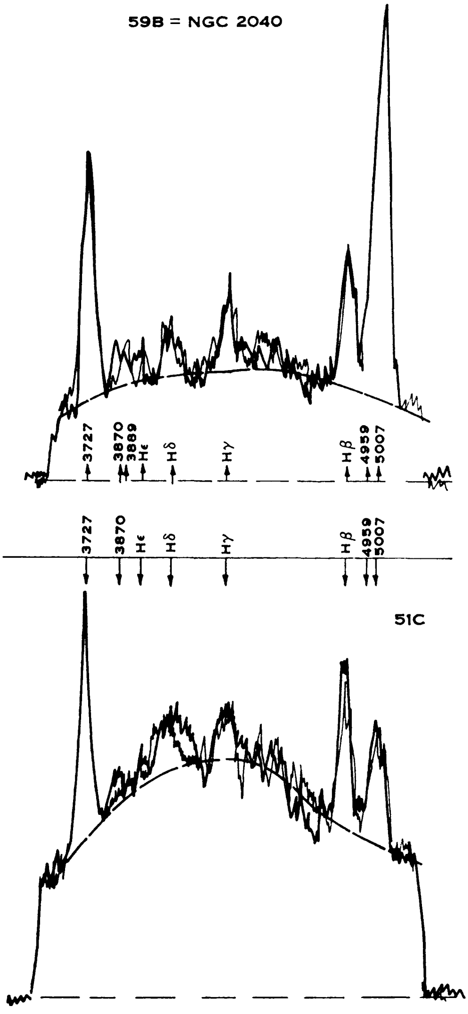

Fig. 5.—Scans of typical emission nebulosities in the Large Magellanic Cloud. ORI filter, 103aE emulsion, 20 min exposure.

described in the literature (see e.g. Aller (1956) or Seaton (1960)). The density of hydrogen can be obtained from the surface brightness if one postulates a uniformly radiating sphere and chooses an electron temperature. For most estimates we choose $T_\epsilon = 10{,}000\,^\circ$K.

For each nebulosity one estimates the radius in seconds of arc from Henize's catalogue. Assuming a distance to the LMC one can then convert this angular radius

Table 2

DATA FOR THE EMISSION NEBULOSITIES IN THE LARGE MAGELLANIC CLOUD

Henize Catalogue Number	Quality of Hβ	Slots (Entrance, Exit)	Estimated Fraction of the Slot Area Filled by Nebulosity	S(Hβ) Surface Brightness	$\frac{I(N_1+N_2)}{I(\mathrm{H}\beta)}$	Excitation Class
5	B	D5–D4	1	0·6	1·5	3
8	B	D5–D4	~ $\frac{3}{8}$	1·7	4·1	4
9	C	D5–D4	1	0·30	2·1	3
11AB	A	D5–D4	1	3·9	4·0	4
11B					4·4	4
11C					4·1	4
11CD	A	D5–E2	~1	3·8	4·5	4
11E		D5–D4	~ $\frac{2}{3}$	0·9	4·0	4
11F	A	D5–D4	1	1·6	2·1	3
11I	C	D5–D4	$\frac{1}{2}$	0·7	2·6	3
17	B	D5–D4	~ $\frac{1}{2}$	0·6	2·0	3
23A	A	D5–D4	~ $\frac{2}{3}$	1·1	2·7	3
30B	C	D5–D4	$\frac{1}{5}$?	3·2	0·8	5
44B	B	D5–D4	~ 1	1·0	1·6	3
44C	B	D5–D4	$\frac{5}{6}$	2·1	6·3	4
44D	A	D4–D4	$\frac{2}{3}$	1·6	1·3	3
44F	B	D4–D4	$\frac{1}{3}$	2·1	1·9	3
51A	B	D0–D4	$\frac{2}{3}$	0·8	1·2	3
51C	A	D5–D4	~ $\frac{5}{8}$	1·6	1·0	3
51D	B	D5–D4	$\frac{2}{3}$	1·1	1·8	3
55	A	D5–D4	1	2·7	2·0	3
57A	B	D5–D4	$\frac{3}{4}$	0·8	1·6	3
59A	B	D5–D4	1	3·3	6·4	4
59B	A	D0–D4	$\frac{2}{3}$	1·3	3·2	3→4
			1 (filled ?)	0·5		
63	B	D5–D4	$\frac{1}{6}$ (intense →)	2·9	2·0	3
68B		D5–D4	(if 1, then →)	0·8		
			(if $\frac{1}{10}$, then →)	8·4	1·6	3
69	A-	D5–D4	(if 1, then →)	1·0		
			(if $\frac{1}{10}$, then →)	9·8	1·4	3
70	C	D5–D4	~1	0·25	1·8	3
77			~1	1·5	I(3727) = 3·7	
79	A	D5–D4	(if 1, then →)	3·4*		
			(if $\frac{1}{4}$, then →)	5·9	3·9	4
79 (north)	A	D0–D4	~1	1·9	1·5	3
83	A	D5–D4	$\frac{5}{8}$	3·4	4·1	4
91	A	D5–D4	$\frac{2}{3}$	2·4	2·2	3
92	C	D5–D4	$\frac{2}{3}$	0·65	2·2	3
103	E	D5–D4	~1	0·65		
105A	A	D5–D4	~1	1·5	2·9	3
113i ABED	A	D4–D4	$\frac{2}{3}$	1·7	1·9	3
113ii	E	D4–D4	~ $\frac{1}{2}$?	0·4	3·4	4
119	A	D5–D4	~1	1·6	1·9	3
120	A	D5–D4	~1	2·4	1·2	3
144	A	D5–D4 D4–D4	~1?	1·7	4·9	4

https://doi.org/10.1017/S007418090005275X Published online by Cambridge University Press

TABLE 2 (*Continued*)

Henize Catalogue Number	Quality of Hβ	Slots (Entrance, Exit)	Estimated Fraction of the Slot Area Filled by Nebulosity	$S(\mathrm{H}\beta)$ Surface Brightness	$\frac{I(N_1+N_2)}{I(\mathrm{H}\beta)}$	Excitation Class
148C	C	D5–D4	$\frac{3}{4}$	0·8	2·1	3
154A	A	D5–D4	$\frac{3}{4}$	2·0	1·9	3
158C	B	D5–D4	$\frac{3}{4}$	1·5	2·8	3
159		D4–D4	$\frac{5}{6}$	1·7	2·5	3
159A	B	D4–D4, D3–D4	$\frac{1}{4}$, $\frac{1}{3}$	4·4	5·8	4
159C	A	D5–D4	1	1·7	3·2	3→4
159D+F	A	D5–D4	$\frac{5}{6}$	1·7	1·9	3
160		D4–D4	~1	3·2	4·4	4
160A		C5–C4	$\frac{2}{3}$	19·0	4·1	4
160A+D		D5–D4	$\frac{5}{6}$	4·5	4·4	4
160B+C	A	D5–D4	~ $\frac{2}{3}$	1·6	3·8	4
163	B	D5–D4	1	0·5	2·0	3
164	B	D5–D4	1	0·7	1·8	3
180	A	D5–D4	$\frac{5}{6}$	1·1	2·4	3

* $\frac{1}{4}$ for the most intense blob.

to radius in centimetres. For this purpose we assumed a distance of 46 kpc. Then

$$r_{\mathrm{neb}} = 6{\cdot}87 \times 10^{17}\ \theta_{\mathrm{n}}'',$$

where θ_{n}'' is the radius in seconds of arc. Then from the measured surface brightness one can calculate the electron density (assuming hydrogen is much more abundant than helium); see e.g. Aller (1954*a*), p. 204. We use, however, the correction to the Boltzmann formula b_4 (10,000 °K) obtained by Burgess (1958). Similar calculations may be carried out for $T_\epsilon = 15{,}000$ °K.

Turning to the forbidden lines of [OII] and [OIII], we may calculate

$$\frac{N(\mathrm{OII})}{N(\mathrm{OIII})} = \frac{I(3727)}{I(N_1 + N_2)}\, P_\epsilon(N_\epsilon, T_\epsilon),$$

where $I(3727)$ is the intensity of 3727 of [OII] and $I(N_1 + N_2)$ is the sum of the intensities of the two green nebular lines. Here $P_\epsilon(N_\epsilon,\ T_\epsilon)$ is a known function of the electron temperature, electron density, and atomic parameters involved in the ground configurations of OII and OIII. For details see Aller (1954*b*) and Seaton and Osterbrock (1957). Similarly (Aller 1954*b*) we can write

$$N(\mathrm{OIII}) = B(N_\epsilon,\ T_\epsilon)\ \frac{I(N_1 + N_2)}{I(\mathrm{H}\beta)},$$

where B can be tabulated as a function of N_ϵ and T_ϵ.

Table 4(*a*) gives the results for an electron temperature of 10,000 °K. Successive columns give the number of the nebula in Henize's catalogue, the electron density (number of electrons cm^{-3}), the number of OIII ions calculated from the ratio $I(N_1 + N_2)/I(\mathrm{H}\beta)$, and the ratio $N(\mathrm{OII})/N(\mathrm{OIII})$ calculated from $I(3727)/I(N_1 + N_2)$.

https://doi.org/10.1017/S007418090005275X Published online by Cambridge University Press

TABLE 3

RELATIVE INTENSITIES (Hβ = 10) IN THE LMC

Nebula No.	[OIII]	N_1+N_2	Hβ	Helium 4472	Hγ	Hδ	3969	3865	3835	[OII] 3727
5	A	15	B 10		E 1·1	E 2·1	E 0·9	E 1		B 15
8	A	41	B 10		C 5	D 3·4	E 1·4	E 2·5		B 20
9	C	21	C 10							D 26
11AB	A	40	A 10	C 0·7	A 4·1	B 1·5	B 1·2	B 2·8		A 16·5
		N_1 N_2								
11B		32 11·5	10							
11C		32 8·6	10							
11CD	A	45	A 10	E 0·6	B 4	B− 2	C 1·4	B− 3·8		B+ 22
11E		40	10	1·7	5·3	4·9	1·1	5·5	2·3	25
11F	A	21	A 10	0·2	C 3·8	D 2·8	E 0·6	E 1·1		A 30
11I	C	26·5	C 10		C 4·4					C 36
17	B	19·5	B 10		D 3·8	E 1·4				B 35
23A	A	27	A 10		D 3·8	D 3·5	E 1·5	E 4·7		(A) 22
30B	C	8	C 10	D 2·5	D 4·4	D 4·9	E 0·6	E 1·6		D 10
44B	B−	16	B 10		D+ 2·5	D− 2·4	E 0·8	E 1·6		A 19
44C	A	63	B 10	E 0·5	B 5	D 2·1	E 1·3	C− 4·1	1·1	A 21·3
44D	A	13	A 10	E 0·8	C 5	D 2·8	E 1·8	E 1·2	E 0·6	A 37
44F	A	19	B 10		D 5	D 1·4	E 1·5	E 1·4		B 34
51A	B	12	B 10		E 3·8	E 1·7				B 35
51C	B	9·7	A 10	E 0·5	B 3·8	D− 3·1	E 1·5	E 2·5		A 37
51D	B	18	B 10							B 21
55	A	20	A 10	E 0·2	B 3·9	C 2·25	D 1·5	D 1·6		A 32
57A	B	16	B 10	E 1·1	D 4·4	E− 4·5	E− 4·1			A 51
59A	A	64	B 10	C 0·7	B 3·8	B 2	C 15	B 2·8		A 13
59B	A	32	A 10	E 1·2	B 5	C 2·8	E 0·9	D 2·7		A 32
63	B	20	B 10	E 1	C 3·8	D 5·6	E 3	E 2·8		B 31
66A										C 14·5
68B		16	10		C 6·9	D 2·8	E 1·5	E 1·1		A 41

TABLE 3 (*Continued*)

69	B+	14	A−	10			B	4·3	C	4·2	D	2·1	D	2·1			A	43
70	C	18	C	10			D	4·3	E	3·8							B	40·5
77		10																3·7
79	A	39	A	10			C	3·8	D	2·5	E	0·6	E	1·2			A	23
79N	A	15	A	10	E	0·5	C	1·9	E	1·4	E	1·5	E	0·8			A	35
83		41	A	10		0·7	B	4	C	2·1	D−	1·1	D−	1·9	E	0·6	A	22
91	A	22	A	10	E	0·7	D	4	D	2·8	E	1·4	E	3·2	E	1·9	A	31
92	B	22	C	10			D	4·5	E	4·2	E	2	E	4			C	19
103			E	10			E	4·6										
105A	A	29	A	10	E	0·35	C	3·5	D	2·1	E	1·5	E	1·6			A	28
113i ABED	A	19	A	10			C	3	D	1·4	E	0·9	E	2·1	E	1	A	29
113ii	E	34	E	10			E?	10									D	44
119	A−	19	A	10	E	0·2	B	3·8	D	2·1	D	1·4	D	3·2			A	27
120	A	12	A	10		0·35	B	4·3	C	2·4	C	2·7					A	33
144	A	49	A	10	E	0·35	C	3·6	D	2·95	D	2	D	5·4			A	23
148C	B	21	C	10			E	4·5	D	5·3							C	28
154A	A	19	A	10	D−	0·95	C	3·4	C	1·7	C	1·4	D	1·3			A	21
158C	A	28	B	10	E	0·8	C	4·8	C	3·4	D	1·4	C	2·7	D	1·4	A	25·5
159		25		10		0·6		3·1		3·1		1·2		3·5				31·5
159A	A	58	B	10	D	0·8	C	4·3	C−	3·9	D	1·6	C−	3·2	E	0·8	A	30
159C	A	32	A	10	D−	0·5	B	4·1	C	1·7	D	0·9	D+	1·4			A	16
159D+F	A	19	A	10	E	0·2	B	4·3	B	2·5	D	1·1	C	1·6			A	30
160		43·5		10		0·8		3·8		1·8		1·5		2·8		0·8		14
		N_1 N_2																
160A		30 10·6		10														
160A+D		43·5		10				3·6		2·4		2		2·4				16
160B+C	A	38	A	10	C	1·9	B	4·6	D+	3·5	E	1·1	D	1·6			A	27
163	B	20	B	10			C−	4·1	E	2	E	0·8	B	2·2			B	25
164	A	18	B	10	E	0·35	C	4·4	D	6·2		1·2					B	28
180	A	24	A	10	E	0·95	B	6·3	B	6	C	1·8	C	3·2			A	31

In order to see what the effects of uncertainty in the electron temperature would be, we also carried out calculations for $T_\epsilon = 15{,}000\,°\mathrm{K}$ (see Table 4(*b*)). The electron density is increased by about 20%. The number of doubly ionized oxygen atoms is cut in half and $N(\mathrm{OII})/N(\mathrm{OIII})$ is reduced to about three-quarters of its value for 10,000 °K.

TABLE 4(*a*)

ELECTRON DENSITIES AND IONIC CONCENTRATIONS FOR T_ϵ = 10,000 °K

Nebula No.	N_ϵ	$N(\mathrm{OIII})$	$\frac{N(\mathrm{OII})}{N(\mathrm{OIII})}$	Nebula No.	N_ϵ	$N(\mathrm{OIII})$	$\frac{N(\mathrm{OII})}{N(\mathrm{OIII})}$
5	8	$0\cdot39 \times 10^{-3}$	1·13	79A	40	$5\cdot00 \times 10^{-3}$	0·68
8	19	2·55	0·56	79E	15·5	0·75	2·65
9	4	0·27	1·35	83	12	1·51	0·61
11AB	17	2·12	0·47	83A	36	4·68	0·61
11CD	22	3·30	0·54	91A+B	25	1·79	1·57
11E	12·5	1·63	0·70	92	9	0·65	1·01
11F	15·5	1·10	1·57	103	6	—	—
11I	14·5	1·20	1·51	105A	10·6	1·10	1·06
17	12·5	0·78	2·00	113i ABED	19	1·19	1·71
23A	15·5	1·37	0·90	113ii	4	0·42	1·44
30B	57	14·4	0·14	119	7	0·39	1·62
44B	18	0·97	1·31	120	20	0·80	3·02
44C	28	5·77	0·38	144	9	2·43	0·52
44D	20	0·87	3·10	148C	12·5	0·85	1·49
44F	27	1·65	2·02	154A	25	1·57	1·24
51A	29	1·12	3·33	158C	36	3·32	1·03
51C	20	0·60	4·32	159	11·6	0·91	1·44
51D	7	0·37	1·31	159A	40	7·80	0·59
55	12·5	0·81	1·82	159C	17	1·73	0·54
57A	21	1·05	3·55	159D+F	17	1·66	1·71
59A	21	4·21	0·22	160	10	1·46	0·34
59B	15·5	1·62	1·13	160A	68	8·84	—
63	5·6	0·33	1·73	160A+D	34	4·98	0·40
63A	40	2·59	1·75	160B+C	22	2·66	0·79
68B	11·6, 98	0·60, 5·1	2·84	163	8	0·50	1·39
69	12·5, 104	0·56, 4·72	3·37	164	8	0·44	1·75
70	3·7	0·23	2·54	180B	9	0·69	1·46

Similarly one may estimate the concentration of ions of Ne^{2+} from the 3868 line. The [NeIII] lines are always relatively weak and are blended with Balmer lines. Hence only rough estimates of their intensities can be extracted from the data. To do this we plot the Balmer decrement from Hβ to Hδ and extrapolate with the aid of the well-known theory to get the expected intensity of λ3868. The difference between the observed and calculated value is then attributed to [NeIII]. We can write (Aller 1954*b*)

$$\frac{N(\mathrm{NeIII})}{N(\mathrm{OIII})} = \frac{I(3868)}{I(N_1+N_2)}\, P_{\mathrm{Ne}}(N_\epsilon,\, T_\epsilon).$$

Numerically $P_{\mathrm{Ne}} = 4\cdot04$ for $T_\epsilon = 10{,}000$ and $3\cdot07$ for $T_\epsilon = 15{,}000\,°\mathrm{K}$.

To obtain the ratios of oxygen and neon to hydrogen we now proceed as follows. Consider first the oxygen problem. Oxygen can exist as OI, OII, and OIII; little is triply ionized. If one plots a histogram of $[N(\text{OII}) + N(\text{OIII})]/N(\text{H})$, he can get an idea of the absolute abundance of oxygen by assuming that the nebulae with the largest values of this ratio would contain oxygen in only these two stages of ionization. In this way one finds the most likely value to be

$$N(\text{O}) = 3{\cdot}0 \times 10^{-4} N(\text{H}),$$

as compared with $4 \times 10^{-4} N(\text{H})$ for the Orion nebula (Aller and Liller 1959).

TABLE 4(*b*)
ELECTRON DENSITIES AND IONIC CONCENTRATIONS FOR $T_\epsilon = 15{,}000\,°\text{K}$

Nebula No.	N_ϵ	$N(\text{OIII})$	$\frac{N(\text{OII})}{N(\text{OIII})}$	Nebula No.	N_ϵ	$N(\text{OIII})$	$\frac{N(\text{OII})}{N(\text{OIII})}$
5	10	$0{\cdot}18 \times 10^{-3}$	0·79	79A	5	$2{\cdot}34 \times 10^{-3}$	0·49
8	23	1·15	0·40	79E	18	0·35	1·85
9	4·5	0·12	0·97	83	15·5	0·72	0·43
11AB	20	0·97	0·32	83A	44	2·24	0·43
11CD	26·5	1·46	0·38	91A+B	31	0·81	1·12
11E	15·5	0·72	0·50	92	10	0·27	0·72
11F	18	0·50	1·12	103	8	—	—
11I	17	0·54	1·06	105A	13·5	0·49	0·76
17	15·5	0·35	1·40	113i ABED	23	0·53	1·21
23A	20	0·63	0·65	113ii	51	0·21	1·03
30B	70	6·88	0·097	119	8	0·18	1·13
44B	23	0·44	0·92	120	24	0·37	2·14
44C	34	2·67	0·27	144	10	0·61	0·38
44D	25	0·40	2·20	148C	15·5	0·38	1·04
44F	33	0·77	1·42	154A	31	0·69	0·88
51A	36	0·53	2·34	158C	43	1·50	0·72
51C	24	0·28	3·04	159	14·5	0·40	1·01
51D	8	0·14	0·92	159A	49	3·47	0·41
55	15·5	0·35	1·28	159C	20	0·73	0·38
57A	25	0·50	2·50	159D+F	22	0·53	1·21
59A	25	0·69	0·16	160	11·6	0·62	0·23
59B	18	0·74	0·79	160A	82	4·32	—
63	6·5	0·15	1·22	160A+D	40	2·57	0·29
63A	51	1·22	1·22	160B+C	26·5	1·21	0·56
68B	14·5, 120	0·27, 2·34	2·00	163	9	0·22	0·99
69	15·5, 127	0·25, 2·04	2·38	164	9	0·18	1·24
70	4·5	0·10	1·80	180B	10	0·32	1·03

For neon the problem is very much more difficult since we observe neon only in one stage of ionization, viz. NeIII. Hence we must estimate $N(\text{NeIII})/N(\text{Ne})$. If we choose nebulae with about the same level of excitation as the Orion nebula and assume that the distribution of atoms among various stages of ionization is the same for Orion and the nebulosities under consideration, we can estimate the abundance of neon. The scatter in the resultant neon abundance is considerable. Most of this must arise from the distribution of atoms among various ionization stages and some of it comes from the uncertainties in the intensities which are guessed in only a very rough way.

We may summarize our results as follows. Let us assume an electron temperature of 10,000 °K. The electron density ranges from 4 electrons cm^{-3} to 70 electrons cm^{-3} in the objects studied, with an average of 19. This value is considerably lower than that found for the Orion nebula or the denser regions in 30 Doradus. The upper limit must be much too low as we have made no allowance for the effects of filamentary structure.

Most nebulae fall in excitation classes 3 or 4. That is, they are comparable with planetary nebulae such as IC 418 or IC 2149 in our own Galaxy (Aller 1956).

For every 10,000 hydrogen atoms we would find the following figures for atoms of other types:

Helium.—No reliable estimate can be obtained from the data herein presented since the helium line intensities are in all instances too uncertain. It is best to adopt Johnson's value for this ratio or that obtained by D. J. Faulkner from a photoelectric spectrophotometric study of the 30 Doradus nebula.

Oxygen.—The range for $N(\text{OII} + \text{OIII})$ is from $1 \cdot 0$ to $4 \cdot 1$. We have adopted a value closer to the upper limit on the assumption that all the oxygen would then be concentrated in these two ionization stages. If the electron temperature is lower than 10,000 °K, the ratio may be higher.

Neon.—The range is from $0 \cdot 07$ to $4 \cdot 3$. For 17 of the 55 nebulosities studied, no measurable line was observed. The range and average values are adopted from the data for the 38 nebulae which were believed to show [NeIII] lines, albeit weak. The average is $N(\text{Neon}) = 1 \cdot 4$. Probably this is much too low as we can imagine that the allowance for the atoms in the lower ionization stages is inadequate. Literally interpreted, the results would suggest that neon is less abundant in the LMC than in our Galaxy.

The conclusion drawn from this investigation is that the abundance ratio of oxygen (and probably neon as well) to hydrogen is possibly slightly lower in the LMC than in our Galaxy. We must stress the uncertainty in this result, however, and urge that more detailed attention be paid the brighter nebulosities, particularly 30 Doradus. Scanner observations should be supplemented by photographic spectroscopy of the fainter lines. In any event the biggest stumbling block is going to be the same as that found in the study of other gaseous nebulae, namely, (1) allowing for the distribution of atoms among various stages of ionization, and (2) allowing for effects of filamentary structure.

The data obtained in this program should be useful for another problem, namely, the total amount of ionized hydrogen in the LMC. The amount of neutral hydrogen and its spatial distribution is being studied by the CSIRO radiophysics group with the large dish at Parkes. Regions of high gas density can readily be found, and it will be interesting to see if most of the ionized hydrogen regions are simply Strömgren spheres. Results obtained with more modest equipment showed that the 30 Doradus region was the focal point of a concentration of gas unequalled by any other known nebula in the local system of galaxies.

To assess the total amount of ionized hydrogen in the LMC, one must obtain isophotic contours of emission nebulosities, calibrate them by the photoelectric data, and obtain electron densities from the surface brightnesses and some plausible geometrical model. Figure 6 illustrates isophotic contours for the nebulosity 11AB in Henize's catalogue as measured on a plate secured with the 74-inch reflector. The projection of the D4 slot is indicated, as well as the size of the analysing slit

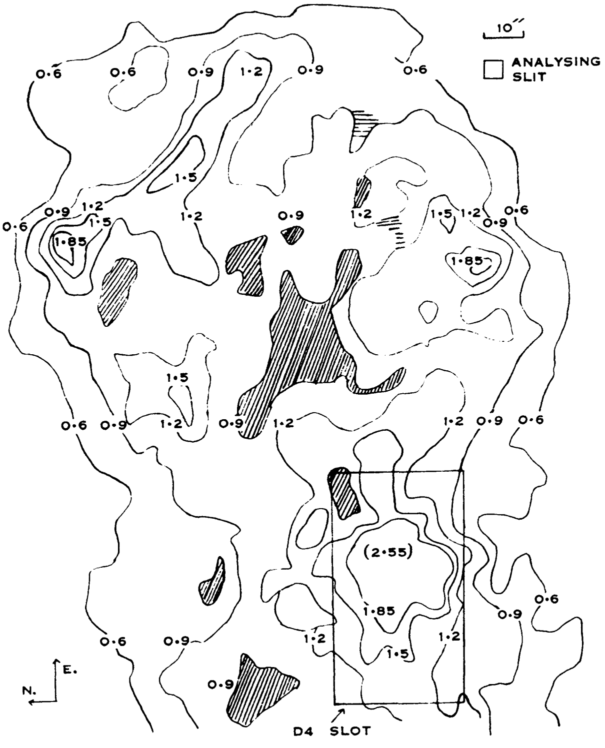

Fig. 6.—30 magnification isophotes, for nebulosity 11AB in Henize's catalogue.

of the isophotometer. Cross-hatching indicates valleys in the isophotes. This program is being extended by one of us (H.R.D.) in an effort to obtain the total mass of ionized hydrogen in the LMC. Photographs secured by Henize (1956) with a 10-inch lens at Lamont-Hussey Observatory in South Africa permit measurement of the fainter nebulosities.

II. The Small Magellanic Cloud

The SMC contains a number of emission nebulosities that are fainter and less conspicuous than those in the LMC. Shapley and Miss Wilson (1925*b*) described 106 nebulosities which have an average diameter of 8 or 10 pc. Nail, Whitney, and Wade (1953) discussed 152 nebulosities in the SMC, while objects tentatively identified by Lindsay (1961) as planetary nebulae are actually diffuse nebulae (Henize and Westerlund 1963). Henize (1956) listed 90 groups of emission nebulosities, some of which were described as separate units, e.g. 84A, 84B, 84C, and 84D.

Table 5 gives data for 12 emission nebulae observed with the 50- and 74-inch reflectors. The first column gives the number in Henize's catalogue and the fourth gives the surface brightness in erg cm^{-2} sec^{-1} steradian^{-1} $\times 10^4$. That is, all surface brightnesses measured ranged from $0 \cdot 3 \times 10^{-4}$ to $3 \cdot 9 \times 10^{-4}$ erg cm^{-2} sec^{-1} steradian^{-1} for H80 and H66 respectively. We obtained them by comparing the nebulae with the southern standard stars, α Gruis, 41 Eridani, and the Oke standard 58 Aquilae.

Table 5

INTENSITIES OF EMISSION LINES OBSERVED IN THE SMALL MAGELLANIC CLOUD

Nebula	θ''	r*	$S(\mathrm{H}\beta)$	N_ϵ (T = 15,000 °K)	E.C.†	N_1+N_2	Hβ	Hγ	Hδ	3969	3865	3727
12A	56	3·9	1·3	20	3	A 45	A 10	B 5·8	C 3·5	D 1·8		B 21
12B	56	3·9	0·5	12	4	A 63	C 10	C 9·9	E 7·3		D 7·9	B 26
19	75	5·2	0·44	10	2	B 21	C 10	D 4·4	E 3·7			B+C 48·5
36	75	5·2	0·66	12	3	A 43	B 10	D 8·9	D 3·9			C 26
37	150	10·4	0·5	7·4	3	A 31	B 10	C 8·8	D 5·3			B 28
76	100	6·9	0·76	11	4	A 76	C 10	C 6·0	D 6·7	D 4·3	C 12·7	C 18
78	56	3·9	0·56	7·7	3	16	10					
80	88	6·0	0·34	8	3	27	10					
83	90	6·2	2·35	21	3	A 33	B 10	B 6·3	C 3·8	D 1·8	D 3·5	B 25
84	80	5·5	0·97	14	3	A 49	A 10	B 7·3	C 4·4	D 2·4	D 8·7	A 54
90	87	6·0	1·6	17	4	A 72	C 10	D 3·1	D 1·7	E 1·0	D 3·2	C 20

* Units of 10^{19} cm.

† Excitation class.

The second column of Table 5 gives the adopted radius of each nebulosity in seconds of arc and the third column gives the corresponding radius in units of 10^{19} cm. Then from the measured surface brightness and an assumed electron temperature of 15,000 °K we derive the density of electrons cm^{-3}. Column 6 gives the excitation class.

The remaining columns give the relative intensities of the principal nebular lines on the scale $I(\mathrm{H}\beta) = 10$. The letters A, B, C, D, etc. denote the estimated reliability of the trace. In each instance, the nebular radiation is superposed on that of background stars which serve to enhance the noise level. The intensity of both Hγ and Hδ appear to have been overestimated in a number of nebulae, possibly because of influence of background stars.

The brightest and largest emission nebula in the SMC is NGC 346 = Henize 66. It is comparable in size with Gum's nebula, the largest known HII region in our Galaxy (Johnson 1961). Measurements of the helium line intensity (Aller and Faulkner 1962) indicated that the He/H ratio was about the same as in the LMC.

Table 6 gives our final intensity values.

TABLE 6
LINE INTENSITIES IN NGC 346

5007	[OIII]	480	4363	[OIII]	6	3889	H, He	20
4959	[OIII]	155	4340	Hγ	50	3865	[NeIII]	60
4861	Hβ	100	4101	Hδ	35	3727	[OII]	140
4471	HeI	3·6	3969	[NeIII]H	36			

If we employ Mathis' expressions (1962),

$$\frac{N(\mathrm{He})}{N(\mathrm{H})} = 1\cdot95\,\frac{I(4471)}{I(\mathrm{H}\beta)},$$

we find $N(\mathrm{He})/N(\mathrm{H}) = 0\cdot070$ in fair agreement with the ratio $0\cdot076$ found for 30 Doradus by Faulkner. Thus the Clouds may be slightly underabundant in He by about 30% as compared with the Galaxy. An intensive spectroscopic study of NGC 346 ought to be carried out to observe weaker lines that may serve to fix the general ionization level and to supply abundance data. The problem of estimating elemental abundances for the ions involves the same difficulties as those previously noted for the LMC.

In summary, the He/H ratio appears to be smaller by about 30% in both Magellanic Clouds than in the Galaxy. The (OII + OIII)/H ratio shows a fair scatter in both Clouds and suggests as a most likely value $N(\mathrm{O})/N(\mathrm{H}) = 3 \times 10^{-4}$. Hence the oxygen and presumably also the neon is most likely underabundant in the Clouds as compared with the Galaxy. In any event the underabundance is not conspicuous.

Acknowledgments

Generous cooperation of the astronomers and technical staff of the Mount Stromlo Observatory is gratefully recalled. We express our appreciation to the National Science Foundation (U.S.A.) whose award of a senior post-doctoral fellowship to one of us (L.H.A.) made his participation in this program possible, to the CSIRO who supported another (D.J.F.) with a graduate fellowship, and to the Air Force

Office of Scientific Research, U.S.A., which through contract number AF 49(638)-807 with the University of Michigan and later with a grant to the University of California, Los Angeles, assisted the program after the observations had been obtained.

References

Aller, L. H. (1954*a*).—"Astrophysics: Nuclear Transformations, Stellar Interiors and Nebulae." (Ronald Press Co.: New York.)

Aller, L. H. (1954*b*).—*Ap. J.* **120**: 401–12.

Aller, L. H. (1956).—"Gaseous Nebulae." (Wiley: New York.)

Aller, L. H., and Faulkner, D. J. (1962).—*P.A.S.P.* **74**: 219–22.

Aller, L. H., and Liller, W. (1959).—*Ap. J.* **130**: 45–56.

Ambartsumian, V. A. (1933).—*Zs. f. Ap.* **6**: 107–13.

Burgess, A. (1958).—*M.N.* **118**: 477–95.

Doherty, L., Henize, K. G., and Aller, L. H. (1956).—*Ap. J.* Suppl. **2**: 345–63.

Henize, K. G. (1956).—*Ap. J.* Suppl. **2**: 315–44.

Henize, K. G., and Westerlund, B. E. (1963).—*Ap. J.* **137**: 747.

Johnson, H. M. (1959).—*P.A.S.P.* **71**: 425–34.

Johnson, H. M. (1961).—*P.A.S.P.* **73**: 20–9.

Lindsay, E. M. (1961).—*A. J.* **66**: 169–85.

Mathis, J. S. (1962).—*Ap. J.* **136**: 374–80.

Nail, V., Whitney, C. A., and Wade, C. M. (1953).—*Proc. Nat. Acad. Sci.* (*Washington*) **39**: 1168–76.

Seaton, M. J. (1960).—*Rep. Progr. Phys.* **23**: 313–54.

Seaton, M. J., and Osterbrock, D. E. (1957).—*Ap. J.* **125**: 66–83.

Shapley, H., and Wilson, H. H. (1925*a*).—Harvard Obs. Circular No. 271.

Shapley, H., and Wilson, H. H. (1925*b*).—Harvard Obs. Circular Nos. 275, 276.

Willstrop, R. V. (1960).—*M.N.* **121**: 17–40.

64. A COMPARISON OF THE 30 DORADUS AND η CARINAE NEBULAE

D. J. Faulkner

Mount Stromlo Observatory

I. Introduction

The program of observations of the 30 Doradus and η Carinae nebulae described here had its origin in the general study of Magellanic Cloud nebulae considered in the previous paper. The 30 Doradus nebula is considerably larger and brighter than the other HII regions in the Clouds, and may be treated in greater detail. The η Carinae nebula was chosen as a comparison object in our own Galaxy.

Most of the results obtained apply to the particular nebulae themselves, and so fall outside the scope of this Symposium. There is one aspect, however, that of the relative abundance of elements in the two systems, which seems to have sufficiently broad implications to warrant inclusion.

II. Observations of the Spectra of the Nebulae

Detailed photoelectric spectrophotometer scans of the blue spectral range were obtained for a bright region in each of the two nebulae. The scanner used was that of the University of Michigan, constructed by Liller (1957). Plates 1 and 2 show